Research article

Ginsenoside-Rp1-induced apolipoprotein A-1 expression in the LoVo human colon cancer cell line

Mi-Yeon Kim [1], Byong Chul Yoo [2],**, Jae Youl Cho [3],*

[1] Department of Bioinformatics and Life Science, Soongsil University, Seoul, Korea
[2] Research Institute and Hospital, National Cancer Center, Goyang, Korea
[3] Department of Genetic Engineering, Sungkyunkwan University, Suwon, Korea

ABSTRACT

Background: Ginsenoside Rp1 (G-Rp1) is a novel ginsenoside derived from ginsenoside Rk1. This compound was reported to have anticancer, anti-platelet, and anti-inflammatory activities. In this study, we examined the molecular target of the antiproliferative and proapoptotic activities of G-Rp1.
Methods: To examine the effects of G-Rp1, cell proliferation assays, propidium iodine staining, proteomic analysis by two-dimensional gel electrophoresis, immunoblotting analysis, and a knockdown strategy were used.
Results: G-Rp1 dose-dependently suppressed the proliferation of colorectal cancer LoVo cells and increased their apoptosis. G-Rp1 markedly upregulated the protein level of apolipoprotein (Apo)-A1 in LoVo, SNU-407, DLD-1, SNU-638, AGS, KPL-4, and SK-BR-3 cells. The knockdown of Apo-A1 by its small-interfering RNA increased the levels of cleaved poly(ADP-ribose) polymerase and p53 and diminished the proliferation of LoVo cells.
Conclusion: These results suggest that G-Rp1 may act as an anticancer agent by strongly inhibiting cell proliferation and enhancing apoptosis through upregulation of Apo-A1.

1. Introduction

Unlike other ginsenosides with various pharmacological activities (e.g., ginsenoside Rg3) [1,2], ginsenoside Rp1 (G-Rp1) is a ginseng saponin artificially prepared from crude ginsenosides (e.g., G-Rg5 and G-Rk1) obtained from *Panax ginseng* Meyer by reduction and hydrogenation [3]. The phytochemical features of G-Rp1 include its chemical stability, and various pharmacological approaches have suggested its value as a biologically active ginsenoside. It has been reported that G-Rp1 is able to prevent skin papillomagenesis induced by 7,12-dimehtylbenz(a) anthracene [4], suppress the proliferation and metastatic processes of cancer cells [5], and reverse multidrug resistance in tumor cells [6]. In addition, G-Rp1 has also been found to block interleukin-1 production and diminish platelet activation and thrombus formation [7,8]. It has also been revealed that G-Rp1 blocks pathways linked to multidrug resistance gene-1 (MRD-1), Src, Akt, and I-kappaB kinase (IKK) in apoptotic and inflammatory processes [6,9,10]. Although these experiments have explored the potential mechanisms underlying the anticancer and anti-inflammatory activities of G-Rp1, the proteins responsible for these pharmacological actions remain unclear. Therefore, in this study, we used proteomic analysis to investigate the effect of G-Rp1 on the protein profiles and expression levels in several cancer cells to understand the mechanisms underlying its anticancer activity.

2. Materials and methods

2.1. Materials

G-Rp1 (Fig. 1) of 97% purity dissolved in 100% dimethylsulfoxide was prepared using established protocols [3]. 3-(4,5-Dimethylthiazol-2-yl)-2,5-diphenyltetrazolium bromide (MTT) and propidium iodide (PI) were purchased from Sigma—Aldrich (St. Louis, MO, USA). Polyvinylidenedifluoride membrane was purchased from

---

* Corresponding author. Department of Genetic Engineering, Sungkyunkwan University, 2066 Seobu-ro, Suwon 440-746, Korea.
** Corresponding author. Research Institute and Hospital, National Cancer Center, 323 Ilsan-ro, Goyang 410-769, Korea.
E-mail addresses: yoo_akh@ncc.re.kr (B.C. Yoo), jaecho@skku.edu (J.Y. Cho).
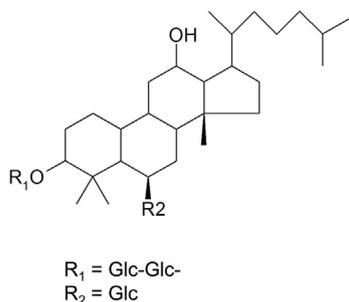
R₁ = Glc-Glc-
R₂ = Glc

Fig. 1. The chemical structure of ginsenoside-Rp1.

Bio-Rad Laboratories, Inc. (Hercules, CA, USA). Phospho- or total antibodies to apolipoprotein (Apo)-A1, cleaved poly(ADP-ribose) polymerase (c-PARP), p85/phosphoinositide 3-kinase, AKT, extracellular signal-regulated kinase (ERK), Src, p65/nuclear factor-κB, p53 and β-actin were purchased from Cell Signaling (Beverly, MA, USA). LoVo, SNU-407, DLD-1, SNU-638, AGS, KPL-4, and SK-BR-3 cells were obtained from the Korean Cell Line Bank (Seoul, Korea).

2.2. Cell lines and culture

LoVo, SNU-407, DLD-1, SNU-638, AGS, KPL-4, and SK-BR-3 cells were maintained in RPMI 1640 medium supplemented with 10% fetal bovine serum (Gibco, Grand Island, NY, USA) and an antibiotic cocktail (100 U/mL penicillin and 100 μg/mL streptomycin), and were subcultured by trypsinization every 3–4 days. Cells were grown at 37°C and 5% CO_2 in humidified air.

2.3. Two-dimensional gel electrophoresis-based comparative proteomics

Two-dimensional gel electrophoresis (2-DE) analysis was performed as described previously [10]. A 0.15-mg protein sample was applied to 13-cm immobilized nonlinear gradient strips (pH 3–10), focused at 8,000 V within 3 hours, and separated on 10% polyacrylamide gels (Serva, Heidelberg, Germany; Bio-Rad). The 2-DE gels were stained with Colloidal Coomassie Blue (Invitrogen, Carlsbad, CA, USA) for 24 hours and then destained with deionized water. Proteins showing abnormal expression were subjected to matrix-associated laser desorption/ionization–mass spectroscopy (MALDI-MS) analysis for identification.

2.4. Cell viability assay

After preincubation of LoVo cells (1×10^6 cells/mL) for 18 hours, G-Rp1 (0–60μM) was added to the cell suspensions and incubated for 24 hours. The cytotoxic effect of G-Rp1 was then evaluated using a conventional MTT assay, as previously reported [11,12]. Three hours prior to culture termination, 10 mL MTT solution (10 mg/mL in phosphate-buffered saline, pH 7.4) was added, and the cells were continuously cultured until termination of the experiment. Incubation was halted by addition of 15% sodium dodecyl sulfate (SDS) into each well, solubilizing the formazan [13]. The absorbance at 570 nm ($OD_{570-630}$) was measured using a Spectramax 250 microplate reader (BioTex, Bad Friedrichshall, Germany).

2.5. Flow-cytometric analysis of DNA fragmentation

Flow-cytometric analysis for PI staining was performed as described previously [14,15]. LoVo (10^6) cells were washed with PBS, fixed in ethanol, suspended in PI solution (1 mg/mL RNase A, 50 micro g/mL PI, and 0.1% Triton X-100 in 3.8mM sodium citrate) and incubated on ice for 30 minutes in the dark. After washing three times with fluorescence activated cell sorting (FACS) buffer, PI fluorescent intensity was analyzed on a FACScan (Becton Dickinson, Franklin Lakes, NJ, USA).

2.6. 2-DE

LoVo cells incubated with G-Rp1 were harvested and suspended in 0.5 mL sample buffer consisting of 40mM Tris, 5M urea (Merck, Darmstadt, Germany), 2M thiourea (Sigma–Aldrich), 4% 3-[(3-cholamidopropyl)dimethylammonio]-1-propanesulfonate (Sigma–Aldrich), 10mM dithiothreitol (Merck), 1mM EDTA (Merck), and a mixture of protease inhibitors (Roche Diagnostics, Basel, Switzerland) for 45 minutes at room temperature. After centrifugation at 16,000 *g* for 15 minutes, 150 μg protein was dissolved in rehydration buffer and applied to both the basic and acidic ends of the 13-cm immobilized pH 3–10 nonlinear gradient strips (Life Technologies, Carlsbad, CA, USA). Proteins were focused at 8,000 V within 3 hours. Immobilized pH gradient strips were rehydrated using 250 μL of each paired preparation. Once isoelectric focusing was completed, the strips were equilibrated in equilibration buffer for 10 minutes. The second dimension was performed using 10% SDS-polyacrylamide gel electrophoresis (PAGE) at 20 mA per gel. The gels were stained using a colloidal blue staining kit (Life Technologies) for 24 hours, and destained with deionized water. Melanie 7.0 software (Swiss Institute of Bioinformatics, Geneva, Switzerland) was used for protein pattern evaluation analysis of the 2-DE gels, as reported previously [16]. Proteins with abnormal levels were subjected to MALDI-MS analysis for identification.

2.7. Mass analysis and data alignment

2-DE gels containing the proteins of interest were excised, destained, and dried in a SpeedVac evaporator (Thermoscientific, Waltham, MA, USA). Dried gel pieces were rehydrated with 30 μL 25mM sodium bicarbonate containing 50 ng trypsin (Promega, Madison, WI, USA) at 37°C overnight. α-Cyano-4-hydroxycinnamic acid (10 mg; AB Sciex, Foster City, CA, USA) was dissolved in 1 mL 50% acetonitrile in 0.1% trifluoroacetic acid, and 1 μL of the matrix solution was mixed with an equivalent volume of sample. Analysis was performed using a 4700 Proteomics Analyzer TOF/TOF system (AB Sciex). The TOF/TOF system was set to positive ion reflect mode. Mass spectra were first calibrated in the closed external mode using the 4700 proteomics analyzer calibration mixture (AB Sciex) and analyzed with GPS Explorer software, version 3.5 (AB Sciex). The acquired MS/MS spectra were searched against SwissProt and NCBI databases using an in-house version of MASCOT.

2.8. Preparation of cell lysates and nuclear fractions for immunoblotting and immunoprecipitation

Cancer cells (5×10^6 cells/mL) were washed three times in cold PBS containing 1mM sodium orthovanadate and lysed in lysis buffer (20mM Tris–HCl, pH 7.4, 2mM EDTA, 2mM ethyleneglycotetraacetic acid, 50mM β-glycerophosphate, 1mM sodium orthovanadate, 1mM dithiothreitol, 1% Triton X-100, 10% glycerol, 10 μg/mL aprotinin, 10 μg/mL pepstatin, 1mM benzimide, and 2mM phenylmethylsulfonyl fluoride) for 30 minutes with rotation at 4°C. The lysates were clarified by centrifugation at 16,000 × *g* for 10 minutes at 4°C and stored at −20°C until needed. Whole cell lysates were then analyzed using immunoblotting analysis [17]. Proteins were separated on 10% SDS-polyacrylamide gels and transferred by electroblotting to a polyvinylidenedifluoride membrane.
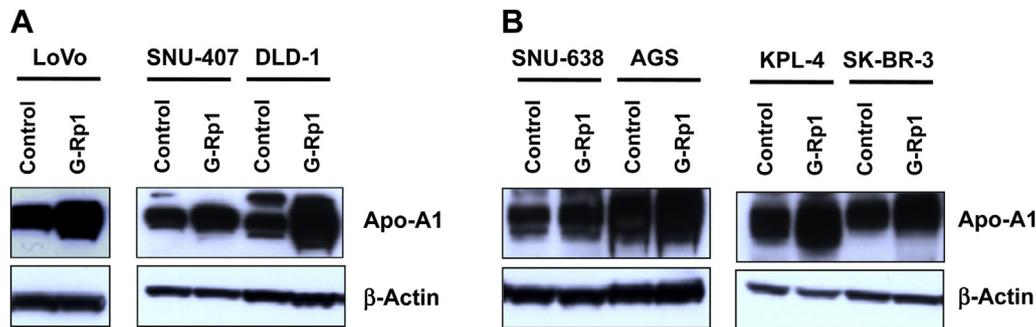
Fig. 2. The effect of G-Rp1 on cell proliferation and DNA fragmentation. (A) LoVo cell proliferation was determined by a conventional MTT assay. (B) Flow-cytometric cell cycle analysis of untreated and G-Rp1-treated cells was performed by propidium iodide staining. LoVo (10^6) cells were exposed to 1.5mM hydroxyurea for 14 hours and then treated with G-Rp1 for 12 hours and 24 hours. Cell samples were analyzed for DNA content by flow cytometry. Data are presented as the mean ± standard error of the mean of three independent observations performed in triplicate. *$p < 0.05$ compared to normal group. G-Rp1 = ginsenoside-Rp1; MTT = 3-(4,5-dimethylthiazol-2-yl)-2,5-diphenyltetrazolium bromide.

Membranes were blocked for 1 hour in Tris-buffered saline containing 3% fetal bovine serum, 20mM NaF, 2mM EDTA, and 0.2% Tween 20 at room temperature. The membranes were incubated for 1 hour with specific primary antibodies at 4°C, washed three times with the same buffer, and incubated for an additional 1 hour with horseradish-peroxidase-conjugated secondary antibodies. The total and phosphorylated levels of Apo-A1, c-PARP, p85/phosphoinositde 3-kinase, AKT, extracellular signal-regulated kinase,

Src, p65/nuclear factor-κB, p53, and β-actin were visualized using an ECL system (Amersham, Little Chalfont, Bucks, UK), as reported previously [18,19].

2.9. Statistical analysis

Data are expressed as the mean ± standard error of the mean. For statistical comparison, results were analyzed using analysis of

Protein Name	Accession No.	Protein MW	Protein pI	Protein Score	Protein Score C.I. %	Total Ion Score	Total Ion C.I. %
Apolipoprotein A-1 (Human)	P02647	30758.9	5.56	68	93.777	31	0

Probability Based Mowse Score

Ions score is -10*Log(P), where P is the probability that observed match is a random event. Protein score greater that 68 are significant (p<0.05).

Fig. 3. Identification of G-Rp1-inducible proteins in LoVo cells. (A) 2-DE gel images showing differential protein levels between normal LoVo or G-Rp1-treated LoVo cells. Enlarged 2-DE gel images demonstrate that the proteins indicated by the white arrows were significantly up-regulated in G-Rp1-treated LoVo cells. (B) Identification of Apo-A1 by MALDI-MS analysis. The protein indicated in Fig. 2A was unambiguously identified as Apo-A1. Mass analysis data are shown in the table. 2-DE = two-dimensional gel electrophoresis; MALDI-MS = Matrix-assisted laser desorption/ionization mass spectrometry; Apo-A1 = apolipoprotein-A1; G-Rp1 = ginsenoside-Rp1.

Fig. 4. Determination of Apo-A1 level in G-Rp1-treated cancer cells. (A, B) Cells were incubated with G-Rp1 for 48 hours. Total levels of Apo-A1 and β-actin in total lysates were determined by immunoblotting analysis. Apo-A1 = apolipoprotein-A1; G-Rp1 = ginsenoside-Rp1.

variance and Student's *t* test. A *p* value < 0.05 was considered statistically significant. All statistical tests were carried out using the computer program STATISTICA version 4.5 (StatSoft Inc., Tulsa, OK, USA).

3. Results and discussion

To understand the mode of action of the antiproliferative and proapoptotic activities of G-Rp1, we first examined whether G-Rp1 was able to block the proliferation of LoVo colorectal cancer cells. As shown in Fig. 2A, G-Rp1 dose-dependently suppressed up to 70% of the proliferation of LoVo cells at 60μM. Although the antiproliferative activity of G-Rp1 in colorectal cancer cells is weaker than in human breast cancer cells [9], the inhibition of LoVo cell proliferation by G-Rp1 indicates that this compound may have common antiproliferative activity regardless of the cell type. Indeed, PI staining strongly implied that the G-Rp1-induced antiproliferative activity was due to the induction of proapoptotic activity by this compound. Thus, G-Rp1 treatment dose- and time-dependently enhanced DNA fragmentation as assessed by PI staining (Fig. 2B), similar to that observed in previous studies [9,20].

Unlike previous approaches that have examined apoptosis-inducing mechanisms of G-Rp1 [20], this study used proteomic analysis to determine the mode of action of G-Rp1. As Fig. 3A depicts, many proteins bands could be detected in LoVo cells using 2-DE. After preparing whole cell lysates with G-Rp1-treated LoVo cells, the blotting patterns between these samples were compared. As shown in Fig. 3A, most band patterns appeared similar, although several bands (indicated with white arrows in Fig. 3A) were strikingly increased in G-Rp1-treated cells. To determine which bands showed higher expression patterns, we further analyzed the biochemical properties of these bands using proteomic analysis. As Fig. 3B indicates, the bands were revealed to be Apo-A1; a major component of high-density lipoprotein that regulates reverse cholesterol transport by modulating the levels of cholesterol and phospholipids in cells [21], and helps control inflammatory responses and oxidative stress [22]. The induction level of Apo-A1 in G-Rp1-treated LoVo cells was also confirmed by immunoblotting analysis of other cancer cells such as SNU-407, DLD-1, SNU-638, AGS, KPL-4, and SK-BR-3. Thus, Fig. 4 clearly indicates that the protein level of Apo-A1 was strikingly enhanced with G-Rp1 treatment, suggesting its involvement in the mechanism of action of G-Rp1.

To evaluate further the regulatory mechanism of G-Rp1-mediated apoptosis, small-interfering (si)RNA for Apo-A1 was introduced into the G-Rp1-treated LoVo cells. As shown in Fig. 5A, c-PARP and p53 were enhanced in siApo-A1-treated cells in the presence of G-Rp1, implying that these proteins might participate in G-Rp1-induced apoptotic activity. Indeed, siApo-A1 treatment
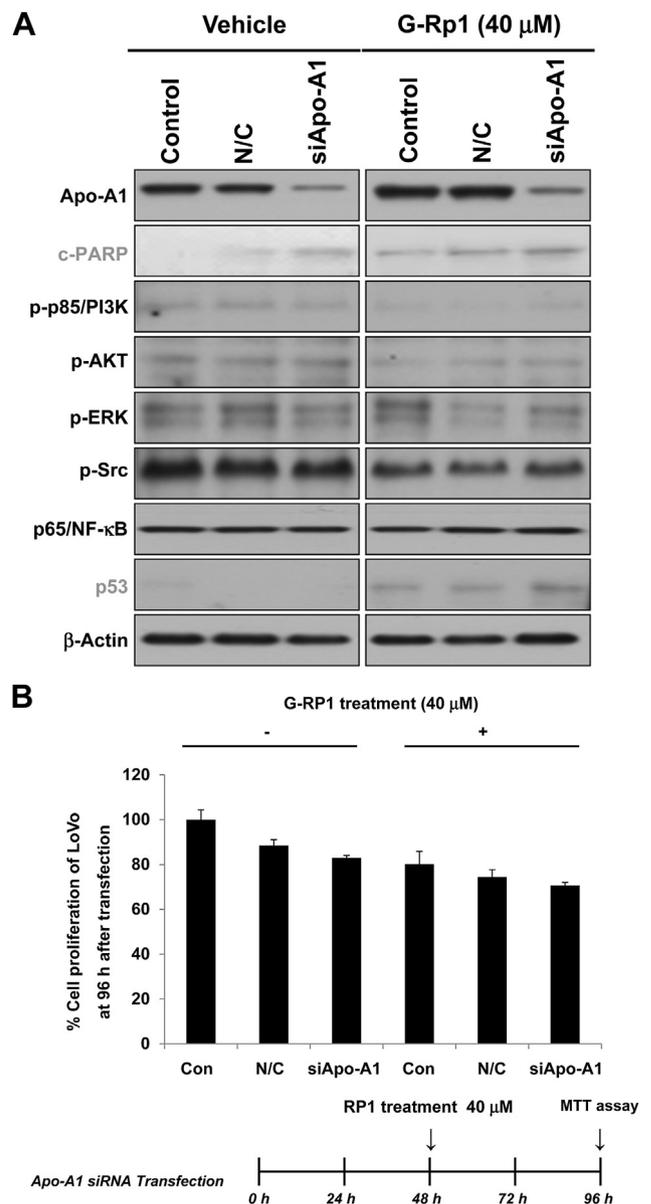

Fig. 5. Effect of siApo-A1 in G-Rp1-treated cancer cells. (A) The effect of siApo-A1 treatment was evaluated by analyzing major signaling molecules and transcription factors in LoVo cells by immunoblotting analysis. (A) The proliferation of siApo-A1-treated LoVo cells was determined by a conventional MTT assay. Data are presented as the mean ± standard error of the mean of three independent observations, performed in triplicate. siApo-A1 = small interfering apolipoprotein-A1; G-Rp1 = ginsenoside-Rp1; MTT = 3-(4,5-dimethylthiazol-2-yl)-2,5-diphenyltetrazolium bromide.
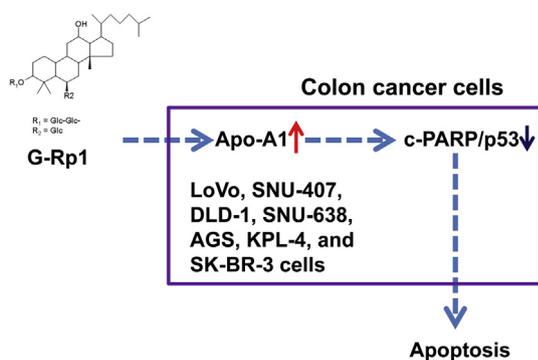
Fig. 6. Schematic diagram of ginsenoside-Rp1 action.

decreased the cell proliferation capacity of LoVo cells, although there was no significant difference (Fig. 5B). Importantly, the level of c-PARP in normal cells under siApo-A1 exposure was clearly upregulated, suggesting that Apo-A1 acts as an apoptosis-preventing protein. Indeed, it was proposed that Apo-A1 might act as a regulator of tumor growth and metastasis [23]. However, considering that Apo-A1 is highly expressed in primary cancer cells rather than just in the secondary state [24], it is possible that this protein is involved in reversing malignant cells back into a normal cycle of differentiation. Recent findings that Apo-A1 is capable of promoting the cardiac differentiation of embryonic stem cells and inducing pluripotent stem cells [25] support this assumption. Therefore, our data and those of previous reports suggest that Apo-A1 is involved in the antiproliferative and proapoptotic activities of G-Rp1, via regulation of cancer cell differentiation. Relevant hypotheses regarding the functional role of Apo-A1 in G-Rp1-mediated anticancer activity will be further tested in upcoming projects.

In summary, we have demonstrated that G-Rp1 is capable of suppressing the proliferation of colorectal cancer cells and enhancing their apoptosis via enhanced levels of Apo-A1. The protein levels of c-PARP and p53 were enhanced under siApo-A1 treatment, therefore, the Apo-A1-mediated anticancer effect of G-Rp1 might be linked to the functional involvement of these proteins, as summarized in Fig. 6. Future studies will examine the exact molecular mechanism of Apo-A1-dependent G-Rp1 pharmacology in terms of its differentiation-inducing activities.

Conflict of interest

The authors report no conflict of interests.

References

[1] Lee B, Sur B, Park J, Kim SH, Kwon S, Yeom M, Shim I, Lee H, Hahm DH. Ginsenoside rg3 alleviates lipopolysaccharide-induced learning and memory impairments by anti-inflammatory activity in rats. Biomol Ther (Seoul) 2013;21:381−90.

[2] Yoo YC, Lee J, Park SR, Nam KY, Cho YH, Choi JE. Protective effect of ginsenoside-Rb2 from Korean red ginseng on the lethal infection of haemagglutinating virus of Japan in mice. J Ginseng Res 2013;37:80−6.

[3] Cho JY, Yoo ES, Baik KU, Park MH, Han BH. *In vitro* inhibitory effect of protopanaxadiol ginsenosides on tumor necrosis factor (TNF)-alpha production and its modulation by known TNF-alpha antagonists. Planta Med 2001;67: 213−8.

[4] Kumar A, Kumar M, Panwar M, Samarth RM, Park TY, Park MH, Kimura H. Evaluation of chemopreventive action of Ginsenoside Rp1. Biofactors 2006;26: 29−43.

[5] Park TY, Park MH, Shin WC, Rhee MH, Seo DW, Cho JY, Kim HM. Anti-metastatic potential of ginsenoside Rp1, a novel ginsenoside derivative. Biol Pharm Bull 2008;31:1802−5.

[6] Yun UJ, Lee JH, Koo KH, Ye SK, Kim SY, Lee CH, Kim YN. Lipid raft modulation by Rp1 reverses multidrug resistance via inactivating MDR-1 and Src inhibition. Biochem Pharmacol 2013;85:1441−53.

[7] Endale M, Lee WM, Kamruzzaman SM, Kim SD, Park JY, Park MH, Park TY, Park HJ, Cho JY, Rhee MH. Ginsenoside-Rp1 inhibits platelet activation and thrombus formation via impaired glycoprotein VI signalling pathway, tyrosine phosphorylation and MAPK activation. Br J Pharmacol 2012;167:109−27.

[8] Kim BH, Lee YG, Park TY, Kim HB, Rhee MH, Cho JY. Ginsenoside Rp1, a ginsenoside derivative, blocks lipopolysaccharide-induced interleukin-1beta production via suppression of the NF-kappaB pathway. Planta Med 2009;75: 321−6.

[9] Kang JH, Song KH, Woo JK, Park MH, Rhee MH, Choi C, Oh SH. Ginsenoside Rp1 from Panax ginseng exhibits anti-cancer activity by down-regulation of the IGF-1R/Akt pathway in breast cancer cells. Plant Foods Hum Nutr 2011;66: 298−305.

[10] Shen T, Lee J, Park MH, Lee YG, Rho HS, Kwak YS, Rhee MH, Park YC, Cho JY. Ginsenoside Rp1, a ginsenoside derivative, blocks promoter activation of iNOS and COX-2 genes by suppression of an IKKbeta-mediated NF-small ka, cyrillicB pathway in HEK293 cells. J Ginseng Res 2011;35:200−8.

[11] Pauwels R, Balzarini J, Baba M, Snoeck R, Schols D, Herdewijn P, Desmyter J, De Clercq E. Rapid and automated tetrazolium-based colorimetric assay for the detection of anti-HIV compounds. J Virol Methods 1988;20:309−21.

[12] Kim MY, Cho JY. 20S-dihydroprotopanaxatriol modulates functional activation of monocytes and macrophages. J Ginseng Res 2013;37:300−7.

[13] Kwon YJ, Jung JJ, Park NH, Ye DJ, Kim D, Moon A, Chun YJ. Annexin a5 as a new potential biomarker for Cisplatin-induced toxicity in human kidney epithelial cells. Biomol Ther (Seoul) 2013;21:190−5.

[14] Du GJ, Wang CZ, Qi LW, Zhang ZY, Calway T, He TC, Du W, Yuan CS. The synergistic apoptotic interaction of panaxadiol and epigallocatechin gallate in human colorectal cancer cells. Phytother Res 2013;27:272−7.

[15] Choi JY, Eo SK. Detection of foreign antigen-specific CD4(+)Foxp3(+) regulatory T cells by MHC class II tetramer and intracellular CD154 staining. Immune Netw 2013;13:264−74.

[16] Cho JH, Lee PY, Son WC, Chi SW, Park BC, Kim JH, Park SG. Identification of the novel substrates for caspase-6 in apoptosis using proteomic approaches. BMB Rep 2013;46:588−93.

[17] Ryoo S, Choi J, Kim J, Bae S, Hong J, Jo S, Kim S, Lee Y. BIRB 796 has distinctive anti-inflammatory effects on different cell types. Immune Netw 2013;13: 283−8.

[18] Lee JA, Lee MY, Shin IS, Seo CS, Ha H, Shin HK. Anti-inflammatory effects of *Amomum compactum* on RAW 264.7 cells via induction of heme oxygenase-1. Arch Pharm Res 2012;35:739−46.

[19] Jung GS, Lee KM, Park JK, Choi SK, Jeon WB. Morphogenetic and neuronal characterization of human neuroblastoma multicellular spheroids cultured under undifferentiated and all-trans-retinoic acid-differentiated conditions. BMB Rep 2013;46:276−81.

[20] Kumar A, Kumar M, Park TY, Park MH, Takemoto T, Terado T, Kitano M, Kimura H. Molecular mechanisms of ginsenoside Rp1-mediated growth arrest and apoptosis. Int J Mol Med 2009;24:381−6.

[21] Taylor AH, Stephan ZF, Steele RE, Wong NC. Beneficial effects of a novel thyromimetic on lipoprotein metabolism. Mol Pharmacol 1997;52:542−7.

[22] Tabet F, Remaley AT, Segaliny AI, Millet J, Yan L, Nakhla S, Barter PJ, Rye KA, Lambert G. The 5A apolipoprotein A-I mimetic peptide displays antiinflammatory and antioxidant properties *in vivo* and *in vitro*. Arterioscler Thromb Vasc Biol 2010;30:246−52.

[23] Zamanian-Daryoush M, Lindner D, Tallant TC, Wang Z, Buffa J, Klipfell E, Parker Y, Hatala D, Parsons-Wingerter P, Rayman P, et al. The cardioprotective protein apolipoprotein A1 promotes potent anti-tumorigenic effects. J Biol Chem 2013;288:21237−52.

[24] Hariprasad G, Hariprasad R, Kumar L, Srinivasan A, Kola S, Kaushik A. Apolipoprotein A1 as a potential biomarker in the ascitic fluid for the differentiation of advanced ovarian cancers. Biomarkers 2013;18:532−41.

[25] Ng KM, Lee YK, Lai WH, Chan YC, Fung ML, Tse HF, Siu CW. Exogenous expression of human apoA-I enhances cardiac differentiation of pluripotent stem cells. PLoS One 2011;6:e19787.